Available online at www.sciencedirect.com
SCIENCE DIRECT®
PERGAMON
International Journal of Heat and Mass Transfer 46 (2003) 3697–3705
International Journal of HEAT and MASS TRANSFER
www.elsevier.com/locate/ijhmt

Stability of a fluid-saturated porous medium heated from below by forced convection

J.P. Kubitschek *, P.D. Weidman

Department of Mechanical Engineering, University of Colorado, UCB 427, Boulder, CO 80309-0427, USA

Received 13 June 2002; received in revised form 5 March 2003

Abstract

A linear stability analysis determining the onset of convection in a bounded rectangular cavity containing a fluid-saturated porous medium is performed for insulated sidewalls, isothermal top wall, and bottom wall heated by forced convection. The nature of the bottom wall heating necessarily involves the Biot number, Bi. Numerical calculations of the critical Rayleigh number, R_c made over the range of Biot numbers $10^{-4} \leqslant Bi \leqslant 10^4$ for cavity aspect ratios $0 \leqslant (a, b) \leqslant 5$ cover all effective bottom heating conditions from the constant heat flux global limit, $R_c = 27.096$ found as $Bi \to 0$ to the isothermal global limit, $R_c = 4\pi^2$ found as $Bi \to \infty$. Marginal stability boundaries, preferred cellular modes and disturbance temperature contours are displayed graphically.

Keywords: Stability; Porous media; Convection

1. Introduction

Many studies of the hydrodynamic stability of fluid-saturated porous media have been pursued to provide improved understanding of geothermal flows, the design of building components for energy conservation, and other heat transfer processes of engineering interest. Lapwood [1] first determined the global minimum Rayleigh number $Ra_{min} = 4\pi^2$ for fluid in a porous medium confined between infinite horizontal surfaces maintained at different uniform temperatures. Beck [2] was the first to report results for a bounded rectangular enclosure with insulating sidewalls. The general result of confinement is flow stabilization, although this effect is weak when either of the box planform dimensions are large compared to the box height.

Nield [3] and Ribando and Torrance [4], *inter alia*, numerically computed the critical Rayleigh number for infinite horizontal plates consisting of an isothermal upper surface and uniform heat flux through the lower surface. In particular, Ribando and Torrance [4] noted that the Rayleigh numbers for an isothermal surface, denoted here as Ra, and for a constant heat flux surface, denoted here as $\widetilde{Ra}$, are equivalently defined at subcritical values; consequently their values at onset of convection may be compared directly. The global minimum value $\widetilde{Ra}_{min} = 27.1$ reported for uniform heat flux represents a 31% reduction of the global minimum value $Ra_{min} = 4\pi^2$ for isothermal heating.

Recently, Wang [5] extended the constant heat flux study to the confined box geometry with insulated sidewalls. The value $\widetilde{Ra}_{min} = 27.096$ reported by Wang [5] provides a more accurate value compared with those found in earlier studies. A significant difference between isothermal and uniform heat flux conditions for the confined geometry lies in the common period λ^* of the doubly periodic spatial grid on which the global minimum values are found. For an isothermal bottom wall $\lambda^* = 1.00H$, while for a bottom wall with uniform heat flux the value reported by Wang [5] is $\lambda^* = 1.35H$, where H is the box height.

Neither uniform temperature nor uniform heat flux boundary conditions are met in engineering practice, though close approximations to them may be realized in controlled laboratory experiments. Use of a variable

* Corresponding author. Tel.: +1-303-445-2148; fax: +1-303-445-6324.
E-mail address: jkubitschek@do.usbr.gov (J.P. Kubitschek).

0017-9310/03/$ - see front matter © 2003 Elsevier Ltd. All rights reserved.
doi:10.1016/S0017-9310(03)00168-6

Nomenclature

a	box dimension along the x-coordinate
b	box dimension along the y-coordinate
Bi	Biot number
$C_{1,2}$	integration constants
g	gravity
h	forced convection heat transfer coefficient
H	box height
k	thermal conductivity of the saturated porous matrix
K	permeability of the porous matrix
$k_{1,2}$	wavenumbers in the x- and y-directions
$\mathbf{k}$	unit vector in z-direction
l	mode number for an isothermal bottom wall
m, n	mode numbers in the x- and y-directions
p	pressure
P	disturbance pressure
$\overline{P}$	base state pressure field
q	bottom boundary heat flux
R	Biot-modified Rayleigh number
Ra	constant temperature Rayleigh number
$\widetilde{Ra}$	constant heat flux Rayleigh number
T	temperature
$\overline{T}$	base state temperature field
ΔT	$T_\infty - T_1$
$\mathbf{u}$	velocity vector
$\overline{\mathbf{u}}$	base state velocity vector
u, v, w	velocity components
U, V, W	disturbance velocity components
$\mathbf{x}$	position vector
x, y, z	Cartesian coordinates

Greek symbols

α	$m\pi/a$
β	$n\pi/b$
γ	$\sqrt{\alpha^2+\beta^2}$
δ	thermal expansion coefficient
Θ	disturbance temperature
κ	thermal diffusivity of the saturated porous matrix
λ	spatial period of minimum critical Rayleigh numbers
μ	dynamic fluid viscosity
ν	kinematic fluid viscosity
ρ	fluid density

Subscripts

c	critical or marginal value
i	indices
min	global minimum value
1	top boundary reference condition
∞	bottom boundary external ambient condition

Superscript

$*$	dimensional variable

heat flux boundary condition involving the Biot number, Bi, to bridge the gap from uniform temperature to uniform heat flux can be traced back (at least) to Carslaw and Jaeger [6] and was introduced in a study of Rayleigh–Bénard convection of a Newtonian fluid by Sparrow et al. [7]. This imperfect boundary condition is sometimes referred to as forced convection heat transfer or Newtonian heating [8]. In a series of papers spearheaded by Kassoy and coworkers [9–11], the effects of imperfect vertical sidewall heating on convection in tall porous slabs was considered to better understand hydrological processes in geothermally active areas. An electronic search of recent literature suggests that the latter studies for a vertical slab and that of Lesnic et al. [8] for a vertical plate are the only porous media investigations that have incorporated Newtonian heating. Surprisingly, we find no porous media investigations that consider imperfect boundary conditions on a horizontal surface, though studies of the preferred pattern of convection in a porous layer with a spatially nonuniform bottom surface temperature have been reported; see for example [12]. In the current investigation we impose the forced convection Robin boundary condition along the bottom surface of a rectangular box containing a fluid-saturated porous medium with isothermal top wall and insulated sidewalls. A linear stability analysis then provides the Rayleigh number and mode configuration at onset of thermal convection for bottom wall thermal conditions ranging from uniform heat flux, found when $Bi \to 0$, to isothermal heating, found in the limit as $Bi \to \infty$. These calculations provide the basis for future nonlinear studies involving realistic bottom wall thermal conditions.

The outline is as follows. From the linearized disturbance equations given in Section 2 we derive the general eigenvalue equation and its limiting Biot number forms in Section 3. Numerical results are displayed in graphical and tabular form in Section 4 and a summary with concluding remarks are given in Section 5.

2. Problem formulation

Consider a fluid-saturated, uniformly porous matrix of height H and rectangular dimensions a^* and b^*. Cartesian coordinates $\mathbf{x}^* = (x^*, y^*, z^*)$ with velocities

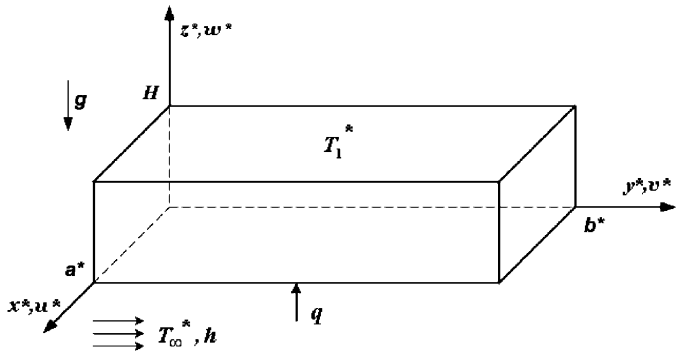

Fig. 1. Bounded fluid-saturated porous medium of height H and rectangular planform dimensions a^*, b^*. The top surface is maintained at constant temperature T_1^* while the bottom surface is heated by forced convection described by the heat transfer coefficient h and the ambient temperature T_∞^*. The vertical sidewalls are assumed to be perfectly insulated.

$\mathbf{u}^* = (u^*, v^*, w^*)$ are employed, as shown in Fig. 1. The vertical sidewalls are insulated and the top wall is maintained at constant temperature T_1^*. The bottom wall is subjected to Newtonian heating with external ambient temperature T_∞^* and convective heat transfer coefficient h.

The governing equations for conservation of mass, momentum and energy in the Darcy–Boussinesq approximation are

$$\nabla^* \cdot \mathbf{u}^* = 0 \tag{1a}$$

$$\mathbf{u}^* = -\frac{K}{\mu}\{\nabla^* p^* + \rho_1 g[1 - \delta(T^* - T_1^*)]\mathbf{k}\} \tag{1b}$$

$$(\mathbf{u}^* \cdot \nabla^*)T^* = \kappa \nabla^{*2} T^* \tag{1c}$$

where p^* and T^* are, respectively, the thermodynamic pressure and temperature; K, the permeability of the porous matrix; μ, the dynamic viscosity of the fluid; ρ_1, the fluid density at top plate reference temperature T_1^*; g, the gravitational acceleration aligned antiparallel to unit vector $\mathbf{k}$; δ, the coefficient of thermal expansion; and κ the thermal diffusivity of the fluid-saturated matrix.

The velocity and thermal boundary conditions are impermeable walls, adiabatic sidewalls, isothermal top plate, and a convectively heated bottom surface, viz.

$$\begin{aligned} &u^* = 0 \ @ \ (x^* = 0, a^*); \quad v^* = 0 \ @ \ (y^* = 0, b^*); \\ &w^* = 0 \ @ \ (z^* = 0, H) \end{aligned} \tag{2a}$$

$$\frac{\partial T^*}{\partial x^*} = 0 \ @ \ (x^* = 0, a^*); \quad \frac{\partial T^*}{\partial y^*} = 0 \ @ \ (y^* = 0, b^*) \tag{2b}$$

$$\begin{aligned} &T^* = T_1^* \ @ \ (z^* = H); \\ &h(T_\infty^* - T^*) = -k\frac{\partial T^*}{\partial z^*} \ @ \ (z^* = 0) \end{aligned} \tag{2c}$$

in which k is the thermal conductivity of the fluid-saturated matrix. The Robin boundary condition at $z^* = 0$ in (2c) states that the external heat flux delivered to the fluid-saturated matrix at its lower boundary is $q = h[T_\infty^* - T^*(0)]$.

Following Wang [5], lengths are normalized with H, velocities with κ/H, pressure with $\kappa\mu/K$, and temperature with qH/k. The only difference between the present normalization and that of Wang [5] lies in the definition of the dimensional heat flux q. In Wang's problem q was a constant to be specified, while in the present case q is calculated from the equation

$$q = \left(\frac{Bi}{1 + Bi}\right)\frac{k\,\Delta T^*}{H} \tag{3}$$

in which $\Delta T^* \equiv (T_\infty^* - T_1^*) > 0$ and Bi is the Biot number defined as

$$Bi = \frac{hH}{k}. \tag{4}$$

Relation (3) is found by eliminating $T^*(0)$ in the bottom wall boundary condition (2c) using the linear temperature profile that exists prior to onset of convection; in this case the bottom wall temperature gradient is identically the uniform base state gradient $\Delta T^*/H$.

The dimensionless boundary-value problem, written in terms of a reduced pressure that removes the hydrostatic component is

$$\nabla \cdot \mathbf{u} = 0 \tag{5a}$$

$$\mathbf{u} = -\nabla p + R(T - T_1)\mathbf{k} \tag{5b}$$

$$(\mathbf{u} \cdot \nabla)T = \kappa \nabla^2 T \tag{5c}$$

$$\begin{aligned} &u = 0 \ @ \ (x = 0, a); \quad v = 0 \ @ \ (y = 0, b); \\ &w = 0 \ @ \ (z = 0, 1) \end{aligned} \tag{5d}$$

$$\frac{\partial T}{\partial x} = 0 \ @ \ (x = 0, a); \quad \frac{\partial T}{\partial y} = 0 \ @ \ (y = 0, b) \tag{5e}$$

$$T = T_1 \ @ \ (z = 1); \quad Bi(T_\infty - T) = -\frac{\partial T}{\partial z} \ @ \ (z = 0) \tag{5f}$$

where $a = a^*/H$ and $b = b^*/H$ are the planform aspect ratios. The remaining dimensionless parameter R that appears in (5b) is the Biot-modified Rayleigh number

$$R = \left(\frac{Bi}{1+Bi}\right)Ra; \qquad Ra = \frac{Kg\delta\Delta T^* H}{\nu\kappa} \tag{6}$$

where $\nu = \mu/\rho_1$ is the kinematic viscosity of the fluid, assumed to be constant. Note that Ra is the traditional porous media Rayleigh number for a cavity with isothermal horizontal plates maintained at uniform temperature contrast ΔT^*.

The conduction base-state solution to the above equations is

$$\begin{aligned} &\overline{\mathbf{u}} = 0; \quad \overline{P}(z) = P_1 - \tfrac{1}{2}R(z-1)^2; \\ &\overline{T}(z) = T_1 - (z-1). \end{aligned} \tag{7}$$

Introducing small disturbances $(\mathbf{U}, P, \Theta)$ for velocity, pressure, and temperature

$$\begin{aligned} &\mathbf{u} = \mathbf{U}; \quad p = \overline{P}(z) + P(x,y,z); \\ &T = \overline{T}(z) + \Theta(x,y,z) \end{aligned} \tag{8}$$

into Eqs. (5a)–(5c) and neglecting quadratically small terms yields the linearized disturbance equations

$$\mathbf{V}\cdot\mathbf{U} = 0; \quad \mathbf{U} = -\nabla P + R\Theta\mathbf{k}; \quad W = -\nabla^2\Theta. \tag{9}$$

The disturbance velocity and temperature boundary conditions obtained from Eqs. (5d)–(5f) are

$$\begin{aligned} &U = 0 \ @ \ (x = 0, a); \quad V = 0 \ @ \ (y = 0, b); \\ &W = 0 \ @ \ (z = 0, 1) \end{aligned} \tag{10a}$$

$$\Theta_x = 0 \ @ \ (x = 0, a); \quad \Theta_y = 0 \ @ \ (y = 0, b) \tag{10b}$$

$$\Theta = 0 \ @ \ (z = 1); \quad Bi\,\Theta - \Theta_z = 0 \ @ \ (z = 0) \tag{10c}$$

where subscripts denote partial differentiation with respect to the subscripted variable.

3. The eigenvalue equation and its limiting forms

Elimination of the vertical velocity W in Eq. (9) gives

$$\nabla^4\Theta + R(\Theta_{xx} + \Theta_{yy}) = 0 \tag{11a}$$

with original and deduced sidewall boundary conditions

$$\begin{aligned} &\Theta_x = \Theta_{xxx} = 0 \ @ \ (x = 0, a); \\ &\Theta_y = \Theta_{yyy} = 0 \ @ \ (y = 0, b) \end{aligned} \tag{11b}$$

and top and bottom wall boundary conditions

$$\begin{aligned} &\nabla^2\Theta = \Theta = 0 \ @ \ (z = 1); \\ &\nabla^2\Theta = Bi\,\Theta - \Theta_z = 0 \ @ \ (z = 0). \end{aligned} \tag{11c}$$

A separable solution satisfying sidewall boundary conditions (11b) is

$$\Theta(x,y,z) = \cos\alpha x \cos\beta y F(z) \tag{12}$$

where $\alpha = m\pi/a$ and $\beta = n\pi/b$. Substitution of (12) into (11a) furnishes the eigenfunction equation

$$\left(\frac{\mathrm{d}^2}{\mathrm{d}z} - \gamma^2\right)^2 F(z) = 0 \tag{13}$$

in which $\gamma^2 = \alpha^2 + \beta^2$. The general solution for $F(z)$ satisfying the $z = 1$ boundary condition (11c) is

$$F(z) = C_1 \sinh[k_1(z-1)] + C_2 \sin[k_2(z-1)] \tag{14}$$

where the constants C_1 and C_2 are arbitrary and

$$k_1 = \sqrt{\gamma\sqrt{R} + \gamma^2}, \quad k_2 = \sqrt{\gamma\sqrt{R} - \gamma^2}. \tag{15}$$

Application of the $z = 0$ boundary conditions (11c) then yields the eigenvalue equation

$$\begin{aligned} &\sin k_2[Bi\sinh k_1 + k_1\cosh k_1] \\ &\quad + \sinh k_1[Bi\sin k_2 + k_2\cos k_2] = 0 \end{aligned} \tag{16}$$

depending explicitly on three parameters: Bi, R and γ. Eq. (16) is valid only for $R > \gamma^2$; a different equation appears when $R < \gamma^2$, but it has no real solutions.

3.1. The large Biot number limit

In the limit of large Bi it is clear that

$$\lim_{Bi\to\infty} R = \lim_{Bi\to\infty}\left(\frac{Bi}{1+Bi}\right)Ra = Ra$$

so the Biot-modified Rayleigh number approaches the classical Rayleigh number for differentially heated horizontal plates. In this case Eq. (16) reduces to the simple form

$$2\sinh k_1 \sin k_2 = 0 \tag{17}$$

and since $k_1 \neq 0$, except for the trivial case $\gamma^2 = 0$, the eigenvalue equation is simply $\sin(k_2) = 0$ with solutions for positive k_2 given by $k_2 = l\pi$ $(l = 1, 2, 3, \ldots)$. Using the definition for k_2 in Eq. (15) yields the eigenvalue relation obtained by Beck [2]

$$Ra = \left(\gamma + \frac{l^2\pi^2}{\gamma}\right)^2. \tag{18}$$

The global minimum value of Ra, found at $l = 1$ and $\gamma = \pi$, is $Ra_c = 4\pi^2$ and these values are located on a doubly periodic planform grid of common spatial period $\lambda = 1.0$ emanating from, but excluding, $a = b = 0$.

3.2. The small Biot number limit

For vanishingly small values of Bi one obtains

$$\lim_{Bi\to 0} R = \lim_{Bi\to 0}\left(\frac{Bi}{1+Bi}\right)Ra = Bi\,Ra = \widetilde{Ra}.$$

In this limit the Biot-modified Rayleigh number R represents the Rayleigh number $\widetilde{Ra}$ for a constant heat flux

bottom wall. Moreover, for vanishingly small Bi, Eq. (16) reduces to the eigenvalue relation obtained by Wang [5]

$$k_1 \cosh k_1 \sin k_2 + k_2 \sinh k_1 \cos k_2 = 0. \tag{19}$$

It is not possible to solve analytically for the global minimum value $\widetilde{Ra}_{\min}$ for this transcendental equation. However, Wang [5] numerically found the value $\widetilde{Ra}_{\min} = 27.096$. He also computed the spatial period $\lambda = 1.35$ of the planform grid on which the global minimum values are found.

4. Results

Eq. (16) is an eigenvalue equation of the form

$$\mathscr{F}(R, Bi, a, b, m, n) = 0$$

that may be evaluated over all modes (m, n) for determining critical values R_c at fixed values of a, b and Bi. We define $R_{\min}$ as the global minimum value of R_c for each fixed value of Bi. In this large parameter space we confined the search to selected values of Biot number in the range $10^{-4} \leqslant Bi \leqslant 10^4$ covering a fine grid of aspect ratios in the range $0 \leqslant (a, b) \leqslant 5$. Figs. 2–4 display the planform variation of R_c for $Bi = 10^{-4}$, 1, and 10^4 plotted both as three-dimensional surface plots and their two-dimensional projections in (a, b)-space. The spatial domains of preferred modes m and n are also displayed.

The projected contours in Fig. 2(b) and the preferred-mode domains in Fig. 2(c) and (d) for $Bi = 10^{-4}$ are in close agreement with the corresponding results given in Figs. 1 and 2 of Wang [5]. The value $R_{\min} = 27.098$ obtained is only slightly higher than the value 27.096 reported by Wang [5] valid for the exact limiting case of uniform heat flux obtained as $Bi \to 0$. Similarly, the projected contours in Fig. 4(b) and the distribution of preferred modes in Fig. 4(c) and (d) for $Bi = 10^4$ are virtually identical to the isothermal bottom wall results given respectively in Figs. 3 and 2 of Beck [2]. The value $R_{\min} = 39.475$ obtained here is only slightly lower than the value of $4\pi^2 = 39.478$ given by Lapwood [1] for the isothermal wall limit. The results in Fig. 3 computed at $Bi = 1$ represent an intermediate situation far removed from the idealized bottom wall boundary conditions studied previously. One can easily observe the increasing complexity of the surface distributions of R_c with increasing Bi. This is reflected in the increased frequency of mode transitions along the a- and b-axes and along the planform diagonal as Bi varies from the constant heat flux limit to the isothermal limit.

Perhaps the best way to interpret the effect of changing the bottom wall boundary condition is to follow the evolution of disturbance isotherms for a given

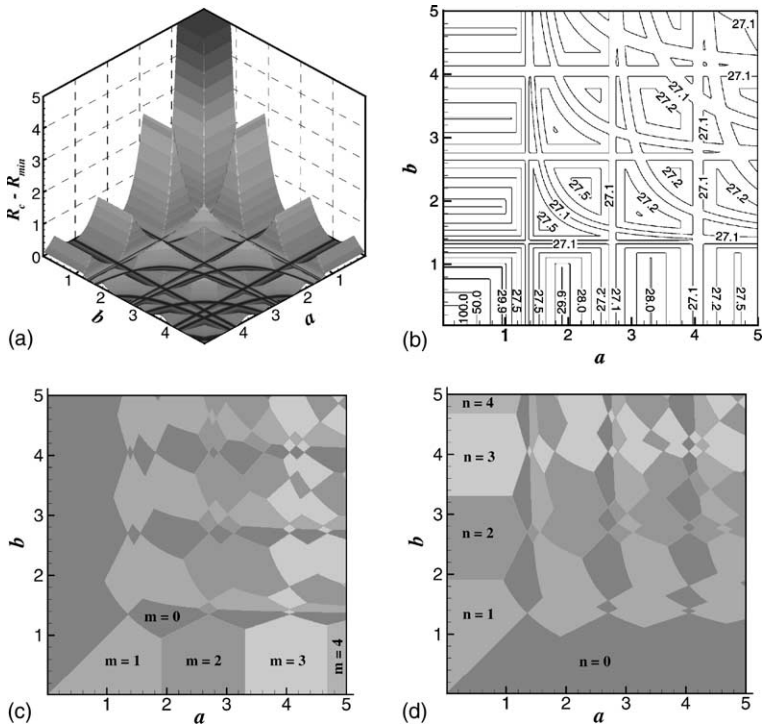

Fig. 2. Critical stability results for $Bi = 10^{-4}$ for which $R_{\min} = 27.098$: (a) marginal stability surface, (b) projection of R_c surface onto the (a, b)-plane, (c) spatial distribution of preferred m-modes, and (d) spatial distribution of preferred n-modes.

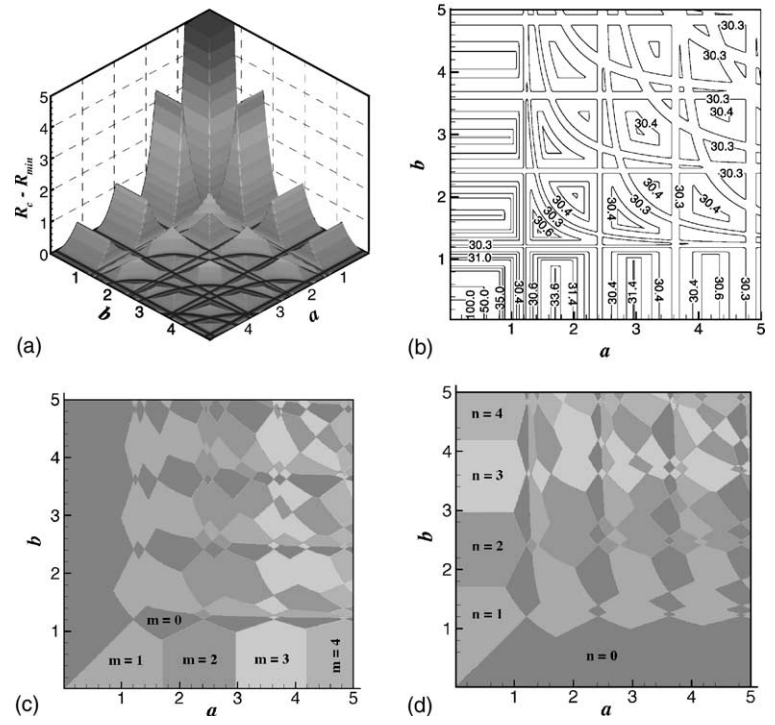

Fig. 3. Same as Fig. 2, but $Bi = 1$ for which $R_{\min} = 30.269$.

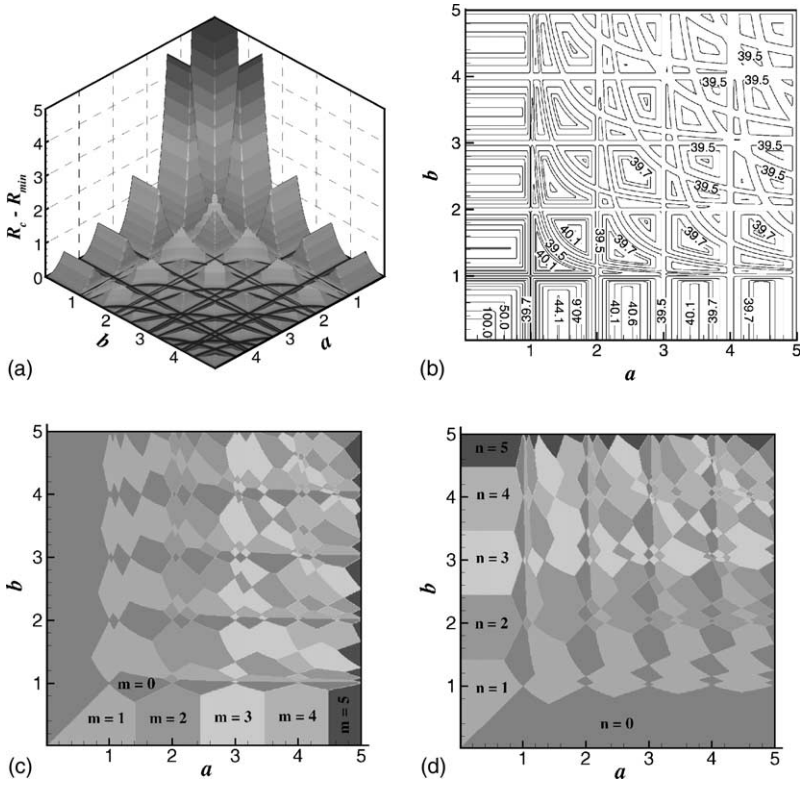

Fig. 4. Same as Fig. 2, but $Bi = 10^4$ for which $R_{\min} = 39.475$.

box geometry as a function of Bi. A short calculation shows that the disturbance temperature field is proportional to

$$\Theta(x,y,z) = \cos\alpha x \cos\beta y[\sin k_2 \sinh\{k_1(z-1)\} + \sinh k_1 \sin\{k_2(z-1)\}]. \quad (20)$$

The results presented in Fig. 5 exhibit top and bottom oblique views of disturbance temperature contours for a square box of dimensions $a = 3$ and $b = 3^-$; this corresponds to the example presented in Fig. 3(a) of Wang [5]. In Fig. 5 hot and cold fluid regions are represented by light and dark shaded areas, respectively. For $Bi = 10^{-4}$ (Fig. 5(a) and (b)) the preferred modes are $m = 2$ and $n = 1$ and the disturbance isotherm patterns are virtually identical to those of Wang [5] for constant heat flux at the bottom wall. The isotherms in Fig. 5(b) clearly reveal the three-dimensional nature of the thermal field showing hot and cold spots on the bottom wall. For $Bi = 1$ (Fig. 5(c) and (d)) the preferred modes flip to $m = 1$ and $n = 2$. Notice the lightest and darkest closed isotherm regions have moved off the bottom wall and reside entirely on the vertical insulated faces. The preferred modes $m = 3$ and $n = 0$ for $Bi = 10^4$ (Fig. 5(e) and (f)) represent a profound change in structure to parallel rolls aligned with the y-axis. The oblique bottom views of the box in Fig. 5(b), (d), and (f) are particularly instructive as they show the bottom wall disturbance temperature field evolving from the variable pattern of high horizontal spatial gradients for $m = 2$ and $n = 1$ through a pattern of weaker spatial gradients at $m = 1$ and $n = 2$, to the zero gradient isothermal surface with roll system $m = 3$ and $n = 0$. Moreover, it is clear the local hot spots on the bottom wall giving rise to vertical plumes can exist only at small Biot numbers that conform closely to a bottom wall condition of uniform heat flux.

The fundamental effect of increasing Bi from the uniform heat flux limit is one of stabilization. The onset of convection is marked by continuously increasing

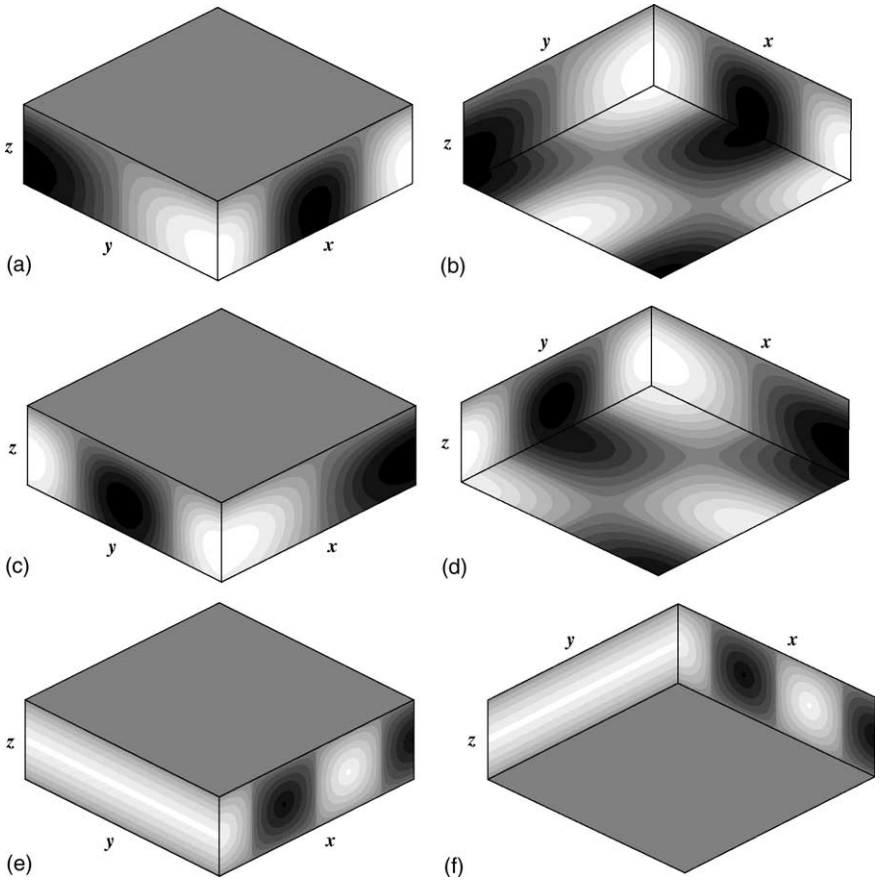

Fig. 5. Top (left column) and bottom (right column) oblique views of disturbance temperature isotherms at onset of convection for a square planform $a = 3$, $b = 3^-$. Subplots (a) and (b) are for $Bi = 10^{-4}$ where $R_{min} = 27.098$ with preferred modes $m = 2$, $n = 1$; (c) and (d) are for $Bi = 1$ where $R_{min} = 30.269$ with preferred modes $m = 1$, $n = 2$; (e) and (f) are for $Bi = 10^4$ where $R_{min} = 39.475$ with preferred cellular modes $m = 3$, $n = 0$.

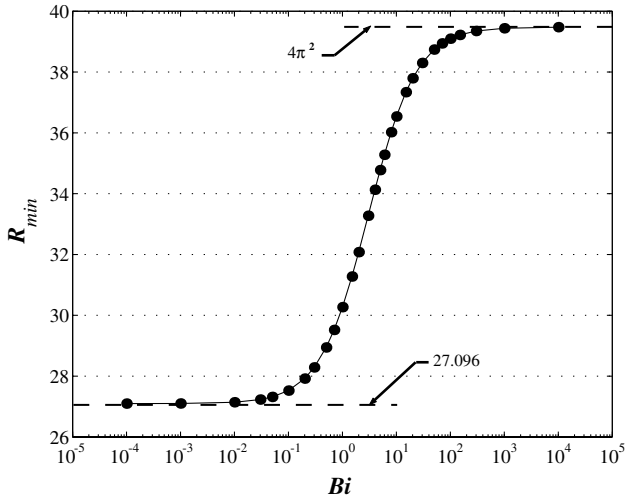

Fig. 6. Computed values of global minimum critical Rayleigh number, $R_{\min}$ as a function of Bi showing the transition between the constant heat flux limit $R_{\min} = 27.096$ computed by Wang [5] and the classical isothermal limit $R_{\min} = 4\pi^2$.

values of $R_{\min}$ displayed in Fig. 6. Here we find that significant deviations (>0.05) from the prescribed heat flux limit $\widetilde{Ra}_{\min}$ and the isothermal limit $Ra_{\min}$ are effectively confined to the Biot number range $0.01 < Bi < 1000$ where the mid-point of transition is very close to $Bi = 3$. Computed values of $R_{\min}$ and the corresponding spatial periods, λ at selected values of Bi are given in Table 1.

Table 1
Global critical Rayleigh numbers $R_{\min}$ and their periodic spacings λ computed at selected values of Bi

Bi	$R_{\min}$	λ
0.0001	27.098	1.350
0.001	27.102	1.350
0.01	27.142	1.348
0.03	27.230	1.343
0.05	27.316	1.339
0.1	27.526	1.328
0.2	27.921	1.308
0.3	28.287	1.291
0.5	28.945	1.261
0.7	29.522	1.238
1.0	30.269	1.209
1.5	31.278	1.174
2.0	32.078	1.149
3.0	33.274	1.116
5.0	34.776	1.080
6.0	35.281	1.069
8.0	36.021	1.055
10	36.538	1.045
15	37.338	1.031
20	37.795	1.024
30	38.298	1.016
50	38.740	1.010
70	38.941	1.007
100	39.097	1.005
150	39.221	1.003
300	39.348	1.001
1000	39.439	1.000
10,000	39.475	1.000

5. Discussion and conclusion

The effect of imperfect bottom heating for a confined fluid-saturated porous medium has been examined. The thermal condition at the lower boundary is characterized by a Biot number measuring the effectiveness of external forced convection. At small, nonzero values of Bi the bottom wall heating is nearly one of uniform heat flux. In this case the well defined disturbance temperature distribution along the bottom boundary is intimately connected to the horizontal cellular structure. The bottom surface however, ultimately becomes an insulated surface when $Bi \equiv 0$. In the other extreme, when Bi becomes large, the forced convective heating from the ambient temperature T^*_∞ is so effective that the bottom wall is essentially an isothermal boundary at that temperature. In this case the bottom boundary disturbance temperature field is no longer linked to the horizontal structure of the cells.

The disturbance isotherm plots in Fig. 5 are particularly revealing. Elevating the Biot number from low values corresponding to uniform bottom wall heat flux to high values corresponding to uniform bottom wall temperature exhibits profound changes in both the preferred modal structure of convection and in the existence and disappearance of thermal plumes. At low Bi hot and cold spots appear at the junction of the vertical walls to the bottom surface and large thermal gradients

exist on both surfaces. As Bi increases, the bottom wall thermal gradients become progressively weaker as bottom wall hot and cold spots migrate continuously to the vertical sidewalls. At high Bi, hot and cold spots can exist only on the vertical sidewalls since the bottom wall tends to an isothermal surface.

This study of forced convective heating of the bottom boundary provides realistic engineering results for the onset of convection in, and heat transfer across, a confined fluid-saturated porous medium of rectangular box geometry at onset of convection. Indeed, all of the global minima are found in the region $27.096 < R_{\min} < 39.478$ but the actual values R_c depend strongly on the planform aspect ratios, especially at low values of a and b. The spatial period λ of the global minimum values found on a rectangular grid in (a, b)-space decreases with increasing Bi. This decrease in spatial period signals the increased complexity of the cellular structure distributions shown in Figs. 2(d), 3(d), and 4(d).

Extensions of this study are numerous. One referee suggested inclusion of imperfect top wall cooling. This would involve a second independent Biot number thereby doubling the parameter space of the problem. One can also envision replacing the vertical insulated walls with imperfectly heated or cooled walls which would introduce yet another independent Biot number. Finally, one may consider each vertical wall exposed to different imperfect heating environments which would break the symmetry of solutions in a box of square planform and greatly increase the parameter space of study. This latter situation is one of general engineering interest. Another problem of considerable engineering interest is the onset of convection in a fluid-saturated porous medium confined in a circular cylinder with axis parallel to gravity. The general situation would be imperfect bottom, top and sidewall heating involving three independent Biot numbers. Solutions of the special case involving imperfect bottom wall heating with isothermal top wall and insulated cylindrical sidewall would provide a continuous bridge across the gap between the uniform temperature bottom wall study of Zebib [13] and the uniform heat flux bottom wall study of Wang [14].

References

[1] E.R. Lapwood, Convection of a fluid in a porous medium, Proc. Camb. Philos. Soc. 44 (1948) 508–521.
[2] J.L. Beck, Convection in a box of porous material saturated with fluid, Phys. Fluids 15 (1972) 1377–1382.
[3] D.A. Nield, Onset of thermohaline convection in a porous medium, Water Resour. Res. 4 (1968) 553–560.
[4] R.J. Ribando, K.E. Torrance, Natural convection in a porous medium: Effects of confinement, variable permeability, and thermal boundary conditions, J. Heat Transfer 98 (1976) 42–48.
[5] C.Y. Wang, Onset of convection in a fluid-saturated rectangular box, bottom heated by constant flux, Phys. Fluids 11 (1999) 1673–1675.
[6] H.S. Carslaw, J.C. Jaeger, Conduction of Heat in Solids, Clarendon Press, Oxford, 1947, pp. 13–14.
[7] E.M. Sparrow, R.J. Goldstein, V.K. Jonsson, Thermal instability in a horizontal fluid layer: effect of boundary conditions and non-linear temperature profile, J. Fluid Mech. 18 (1964) 513–528.
[8] D. Lesnic, D.B. Ingham, I. Pop, Free convection boundary-layer flow along a vertical surface in a porous medium with Newtonian heating, Int. J. Heat Mass Transfer 42 (1999) 2621–2627.
[9] P.D. Weidman, D.R. Kassoy, The influence of side wall heat transfer on convection in a confined saturated porous medium, Phys. Fluids 29 (1986) 349–355.
[10] D.E. Chelghoum, P.D. Weidman, D.R. Kassoy, The effect of slab width on the stability of natural convection in confined saturated porous media, Phys. Fluids 30 (1987) 1941–1947.
[11] M. Wang, D.R. Kassoy, P.D. Weidman, Onset of convection in a vertical slab of saturated porous media between two impermeable conducting blocks, Int. J. Heat Mass Transfer 30 (1987) 1331–1341.
[12] D.N. Riahi, Preferred pattern of convection in a porous layer with a spatially non-uniform boundary temperature, J. Fluid Mech. 246 (1993) 529–543.
[13] A. Zebib, Onset of natural convection in a cylinder of water saturated porous media, Phys. Fluids 21 (1978) 699–700.
[14] C.Y. Wang, Onset of convection in a fluid-saturated porous medium inside a cylindrical enclosure bottom heated by constant flux, Int. Commun. Heat Mass Transfer 25 (4) (1998) 593–598.